

Is the quantum Rabi model adequate in circuit QED for any atom-resonator coupling?

Vladimir E. Manucharyan

*Department of Physics, Joint Quantum Institute,
and Center for Nanophysics and Advanced Materials,
University of Maryland, College Park, MD 20742, USA.*

Alexandre Baksic

Department of Physics, McGill University, 3600 rue University, Montreal, Qc H3A 2T8, Canada.

Cristiano Ciuti

*Laboratoire Matériaux et Phénomènes Quantiques,
Université Paris Diderot, CNRS UMR 7162, Sorbonne Paris Cité,
10 rue Alice Domon et Leonie Duquet 75013 Paris, France.*

(Dated: June 16, 2022)

In circuit quantum electrodynamics (circuit QED), an artificial "circuit atom" can couple to a quantized microwave radiation much stronger than its real atomic counterpart. The celebrated quantum Rabi model describes the simplest interaction of a two-level system with a single-mode boson field. When the coupling is arbitrary large, the bare multilevel structure of a realistic circuit atom cannot be ignored even if the circuit is strongly anharmonic. We explored this situation theoretically for flux (fluxonium) and charge (Cooper pair box) type multi-level circuit atoms at maximal frustration and identified which spectral features of the quantum Rabi model survive and which are renormalized for arbitrary large coupling. In particular, we provide a quantitative comparison with the ideal quantum Rabi model by inspecting not only the circuit energy level spectrum, but also the entanglement spectrum. Despite significant renormalization of the low-energy energy spectrum in the fluxonium case, the key quantum Rabi feature – nearly-degenerate vacuum consisting of an atomic state entangled with a multi-photon field – appears in both types of circuits when the coupling is sufficiently large. Like in the quantum Rabi model, for very large couplings the entanglement spectrum is dominated by only two, nearly equal eigenvalues, in spite of the fact that a large number of bare atomic states are actually involved in the atom-resonator ground state. We interpret the emergence of the vacuum two-fold degeneracy in both circuits as an environmental suppression of flux/charge tunneling due to their dressing by virtual low-/high-impedance photons in the resonator. For flux tunneling, the dressing is nothing else than the shunting of a Josephson atom with a large capacitance of the resonator. Suppression of charge tunneling appears to have the same origin as the dynamical Coulomb blockade of transport in tunnel junctions connected to resistive leads.

I. INTRODUCTION

In the last decade, the field of circuit quantum electrodynamics (circuit QED) [1, 2] has emerged as a frontier of quantum information science thanks to the simultaneous combination of scalable fabrication, strong interactions, and high-coherence offered by superconducting circuits [3]. In both circuit QED and cavity QED [4], the resonant coupling between a single photon and a two-level atom is quantified by the so-called vacuum Rabi frequency g , which is typically orders of magnitude smaller than the photon frequency ω_r and atom transition frequency ω_a . Such a system is then well described by the Jaynes-Cummings Hamiltonian [5], which is the rotating-wave approximation of the celebrated quantum version of the Rabi model [6, 7]. However, in situations where the $g \sim \omega_r, \omega_a$, those systems cannot be accurately described by the Jaynes-Cummings model and one needs to consider the quantum Rabi model. The Hamiltonian corresponding to this model reads:

$$H_{\text{Rabi}}/\hbar = \omega_r a^\dagger a + \frac{\omega_a}{2} \sigma_z + g(a + a^\dagger) \sigma_x, \quad (1)$$

where a^\dagger is a bosonic creation operator for a single electromagnetic mode with a quantum of energy $\hbar\omega_r$. The boson mode is linearly coupled to a two-level system whose algebra is described by the Pauli matrices $\sigma_x, \sigma_y, \sigma_z$. In spite of its apparent simplicity, the exact analytical solution of the quantum Rabi model has been found only recently [8].

An intriguing property of the quantum Rabi model (Eq. 1) in the ultrastrong coupling regime, i.e. when the condition $g \ll \omega_r$ is violated, is the emergence of a non-trivial ground state [9–13], which is not the ordinary vacuum. In the standard scenario of cavity QED, while the excitations are entangled states of the atom and resonator, the ground state is the standard vacuum, namely the product of the zero photon Fock state and the atomic ground state. Instead, in the quantum Rabi model at large couplings the ground state asymptotically becomes a Schrödinger cat state maximally entangled with the atom for increasing coupling [10, 14]. The first excited state tends to an orthogonal entangled atom-cat state. Moreover, the frequency gap between these two non-classical states decreases exponentially with increasing coupling. A qubit consisting of these two entangled atom-resonator states is expected to enjoy protection with respect to a class of decoherence channels and might have applications in quantum information [15].

In a recent experiment [16], an effective quantum Rabi dynamics with arbitrarily large coupling has been realized by using digital quantum simulation techniques [17] with time-dependent drives in a conventional circuit QED system with a relatively small vacuum Rabi coupling. In that driven configuration, one can realize states sharing distinctive properties of the quantum Rabi model eigenstates. Can one implement $g/\omega_r \gg 1$ in a system with a time-independent Hamiltonian? This is of course forbidden for real atoms due to the small value of the fine structure constant. Interestingly, artificial circuit atoms do not suffer from this limitation partly due to the possibility of direct interconnection of circuits by wires [18]. Several groups utilized this approach and reported spectroscopic signatures of a regime where $g/\omega_r \sim 1$ with a superconducting flux qubit coupled to low-impedance resonant modes [19–21].

Here we consider theoretically time-independent analog circuit implementations of the quantum Rabi model for arbitrary strong coupling. When the coupling largely exceeds both the photon and bare two-level transition frequencies, one might wonder if the quantum Rabi model can adequately describe a circuit QED system. In particular, we address the two following problems. First, atom-photon interaction necessarily comes with " A^2 "-like term (terms quadratic in the photon operators), which can be safely neglected for the case of a single artificial atom and $g/\omega_r \ll 1$. This procedure instead is not straightforward once this condition is violated, as it has been for example considered for the Dicke-like problem of $N \gg 1$ artificial, identical atoms coupled to the same resonator mode [10, 22–26] (one of the inherent difficulties of the collective coupling of N artificial atoms is the plain fact that an exact diagonalization of the circuit Hamiltonian including all relevant levels of the artificial atoms is not feasible for $N \gg 1$). Second, artificial circuit atoms do have more than two levels. Even at $g/\omega_r \ll 1$ one must take higher circuit levels into account, for instance, to obtain correct dispersive shifts in the circuit QED in second order in g/ω_r . One can imagine that higher levels are even more important when $g/\omega_r \gg 1$. However, both questions remained largely unexplored in the previous studies investigating one circuit atom coupled to resonator mode [18, 27]. In this paper, we have identified which properties of the quantum Rabi model survive and which ones are modified when considering a multilevel circuit atom with arbitrary large coupling to a lumped-element single-mode resonator.

The manuscript is organized as follows. In Sec. II, as a prelude we consider the coupling between two linear LC -circuits and show that a regime $g \sim \omega_r$ can be naturally achieved with conventional circuit elements by an appropriate interconnection choice. We describe this system both in the flux and charge gauge. We show that the corresponding second quantization Hamiltonian is equivalent to the Hopfield Hamiltonian for semiconductor polaritons [9, 28]. In Sec. III, we introduce the Hamiltonian theory for a multilevel circuit atom arbitrarily strongly coupled to a single-mode lumped-element resonator. In particular, we separately consider the case of a fluxonium [29] artificial atom, which is based on the flux tunneling in and out of a superconducting loop and a Cooper pair box [30] artificial

atom, which is based on charge tunneling in and out of a superconducting island. Fluxonium results are qualitatively applicable to the flux qubit, while the Cooper pair box analysis covers the transmon qubit [31] as well. In both cases, we explore numerically (Sec. IV) the behavior of the transition spectrum, the vacuum degeneracy, and the atom-photon entanglement, drawing a comparison with the ideal two-level quantum Rabi model. We also provide a physical interpretation of the ultrastrong coupling regime, $g/\omega_r \gg 1$, in terms of environmental suppression of flux and charge tunneling [32, 33]. Conclusions and perspectives are summarized in Sec. V.

II. PRELUDE: HOW STRONG CAN THE COUPLING BETWEEN TWO LINEAR CIRCUITS BE?

A minimal circuit model illustrating circuit-circuit interaction consists of a parallel combination of a capacitor C_1 and an inductor L_1 shunted by a series combination of a capacitor C_2 and an inductor L_2 (Fig. 1a,b). Taking the two generalized fluxes ϕ_1 and ϕ_2 in the two capacitors [34], as the generalized coordinates, the circuit Hamiltonian is given by:

$$H_{\text{flux}} = Q_1^2/2C_1 + Q_2^2/2C_2 + \phi_1^2/2L_1 + (\phi_1 - \phi_2)^2/2L_2. \quad (2)$$

Here Q_1 and Q_2 are the conjugate momenta for ϕ_1 and ϕ_2 , respectively. They obey the commutation relation $[\phi_i, Q_j] = i\hbar\delta_{ij}$. Physically, Q_1 and Q_2 are the displacement charges on the plates of the two capacitors C_1 and C_2 . With this choice of circuit variables, the two LC -oscillators are inductively coupled via the term $\phi_1\phi_2/L_2$. We thus call this choice of circuit variables a *flux gauge*. Note that the coupling term does not contain any apparent small parameter. One can also write the Hamiltonian in a different gauge, by applying a unitary transformation $U = \exp(-iQ_2\phi_1/\hbar)$, which displaces $Q_1 \rightarrow Q_1 + Q_2$ and $\phi_2 \rightarrow \phi_2 + \phi_1$, obtaining

$$H_{\text{charge}} = (Q_1 + Q_2)^2/2C_1 + Q_2^2/2C_2 + \phi_1^2/2L_1 + \phi_2^2/2L_2. \quad (3)$$

In this so-called *charge gauge* the circuit-circuit coupling is given by the capacitive term Q_1Q_2/C_1 and again it does not apparently contain a small parameter.

Already at this stage, it is interesting to note that the coupling between these two circuits cannot be classified as inductive or capacitive: clearly this is just a matter of a gauge choice which cannot affect the observables, such as frequencies of the normal modes. To understand the circuit-circuit coupling further we quantize both Hamiltonians. This is done by introducing creation and annihilation operators for the unperturbed modes

$$\phi_j = \sqrt{\frac{\hbar Z_j}{2}}(a_j + a_j^\dagger) \quad (4)$$

$$Q_j = i\sqrt{\frac{\hbar}{2Z_j}}(a_j^\dagger - a_j) \quad (5)$$

where we have introduced mode impedances $Z_{1,2}$ according to the Table II. The resulting flux-gauge Hamiltonian is

$$H_{\text{flux}}/\hbar = \omega_1 a_1^\dagger a_1 + \omega_2 a_2^\dagger a_2 - G(a_1^\dagger + a_1)(a_2^\dagger + a_2) + D(a_1^\dagger + a_1)^2. \quad (6)$$

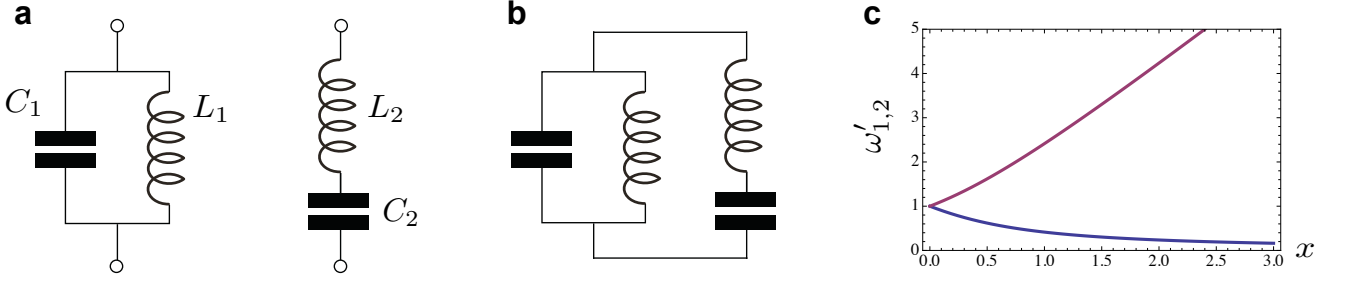
The first term of the Hamiltonian is simply the harmonic oscillator energy of the parallel LC circuit when its terminals are left open. Similarly, the second term is the energy of the series LC circuit when its terminals are connected to each other. The G -term represents the linear coupling between the two LC -modes. The D -term renormalizes the bare parallel LC -mode. Examination of the two constants (Table II) reveals an important dimensionless parameter x that determines the strength of the coupling:

$$x = \frac{1}{2}\sqrt{Z_1/Z_2}. \quad (7)$$

The Hamiltonian (6) has actually precisely the same form that the Hopfield Hamiltonian [9, 28, 35, 36], and the D -term is the circuit analog of the diamagnetic " A^2 -term" of the Hopfield model. We can quantize the charge-gauge Hamiltonian following exactly the same procedure to obtain (see Table II for parameters)

$$H_{\text{charge}}/\hbar = \omega_1 a_1^\dagger a_1 + \omega_2 a_2^\dagger a_2 + \tilde{G}(a_1^\dagger - a_1)(a_2^\dagger - a_2) + \tilde{D}(a_2^\dagger + a_2)^2. \quad (8)$$

ω_1	Z_1	ω_2	Z_2	x	G	D	\tilde{G}	\tilde{D}
$1/\sqrt{L_1 C_1}$	$\sqrt{L_1/C_1}$	$1/\sqrt{L_2 C_2}$	$\sqrt{L_2/C_2}$	$\frac{1}{2}\sqrt{Z_1/Z_2}$	$\omega_1 \times x$	$\omega_1 \times x^2$	$\omega_2 \times x$	$\omega_2 \times x^2$

TABLE I. Parameters of the minimal model of coupling of two LC circuits.FIG. 1. (a) A parallel (left) and a series (right) single-mode resonance LC circuit. (b) Coupled circuits obtained by connecting parallel and series circuits with wires. (c) The two normal mode frequencies of the circuit shown in (b) for identical bare frequencies as a function of the dimensionless coupling parameter x (see Table 1).

Let us assume for the sake of clarity that the two bare frequencies are identical, namely $\omega_1 = \omega_2 = \omega_0$. As it must be, in this case it is particularly apparent that the two Hamiltonians in both gauges have the same normal mode frequencies $\omega'_{1,2}$. Exact diagonalization gives

$$\omega'_{1,2}(x) = \omega_0(\sqrt{1+x^2} \pm x). \quad (9)$$

In the weak coupling regime, $x \ll 1$, we can ignore the D -term and recover a familiar normal mode splitting $\omega'_{1,2} \approx \omega_0 \pm G$. In the opposite limit, $x \gg 1$, the D -term must be taken into account, and we obtain that while the higher mode frequency continues to grow linearly with the coupling as $\omega'_1 \approx 2G$, the lower mode frequency now vanishes algebraically with G as $\omega'_2 \approx \omega_0^2/2G$. Note that despite being small, ω'_2 never reaches zero (Fig. 1c).

We can now clearly see why it is so easy to go beyond weak coupling regime with circuits. Indeed, to make $x \sim 1$ it is sufficient to simply connect two circuits with identical inductances and capacitances! Adjusting circuit elements such that $Z_1 \gg Z_2$ will enhance the coupling even further, making $x \gg 1$. In practice, the range of experimentally achievable circuit impedances is quite large. The lowest impedance of an electromagnetic oscillator is usually limited by the vacuum impedance $Z_{\text{vac}} = \sqrt{\mu_0/\epsilon_0} \approx 377 \, \Omega$, where ϵ_0 and μ_0 are the permittivity and permeability of the free space, respectively. On-chip microstructures often have impedance closer to $50 \, \Omega$ due to geometry and high dielectric constant substrates. To obtain high-impedance, one needs to increase the effective μ_0 . Impedance in excess of resistance quantum (for Cooper pairs) $R_Q = h/(2e)^2 \approx 6.5 \, k\Omega$ was achieved using a kinetic inductance of a Josephson junction chain while maintaining high coherence and showing no spurious resonances [29]. It is therefore relatively straightforward to achieve $x > 5$.

We conclude this section with two important remarks.

First, the two normal modes have a simple electrical engineer's interpretation in the ultra-strong coupling regime $x \gg 1$. The higher frequency mode can be understood as a resonance between L_1 and C_2 (current through L_1 and voltage across C_2 are neglected), while the lower frequency mode can be similarly understood as a resonance between C_1 and L_2 (current through C_1 and voltage across L_2 are neglected). In other words, the two circuits "exchange" their circuit elements such that the largest L pairs up with the largest C and the smallest L pairs up with the smallest C , thus creating a large splitting in the two normal modes in the ultrastrong coupling regime.

Second, introducing a weak Kerr-like non-linearity to one of the oscillators will not modify the normal modes significantly, even if the coupling is strong. Indeed, let us assume that the inductance L_1 is slightly non-linear, i.e. there is a term quartic in ϕ_1 in the energy. Such a non-linearity is typical for a transmon qubit [31]. As remarked above, in the ultra-strong coupling regime, $x \gg 1$, the lower mode is predominantly confined to the inductance L_1 and capacitance C_2 . Therefore, a weak non-linearity in L_1 would simply translate into a weak anharmonicity of the lower mode. Moreover, the higher mode, being predominantly confined to inductance L_2 and capacitance C_1 would be unaffected by such a non-linearity in this (arguably very coarse) approximation. Investigation of more relevant circuit non-linearity, associated with flux/charge tunneling, is the main subject of this paper.

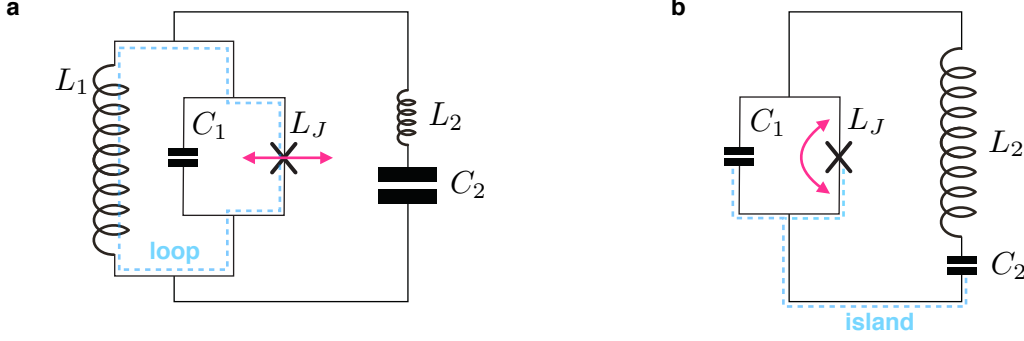


FIG. 2. (a) The circuit scheme for the fluxonium-resonator system considered in Sec. III A, where the cross symbol represents a Josephson junction. The depicted loop is pierced by an external flux ϕ_{ext} (not shown). The main dynamics in this circuit is due to tunneling of flux in and out of the loop through the junction. (b) The circuit for the Cooper pair box case treated in Sec. III B. The depicted island can be additionally voltage-biased (not shown) to create an offset charge Q_{ext} . The main dynamics here is the tunneling of a charge in and out of the island across the junction.

III. CIRCUIT THEORY OF ARBITRARY STRONG ATOM-PHOTON INTERACTIONS

In this section we will describe the coupling of two types of circuit atoms - fluxonium and Cooper pair box - to a single mode LC -resonator, that we will refer to as photon (Fig. 2).

A. Fluxonium atom

To maximize the fluxonium-photon coupling we keep the series L_2C_2 -oscillator from (Fig. 1b) and add a Josephson junction with the Josephson inductance L_J in parallel with the inductance L_1 (Fig. 2a). The loop formed by the junction and the linear inductance L_1 is pierced by the externally applied flux ϕ_{ext} . Introducing the superconducting flux quantum $\Phi_0 = h/2e$, we can write the uncoupled fluxonium atom Hamiltonian as

$$H_{\text{fluxonium}}(\phi_1, Q_1) = Q_1^2/2C_1 + \phi_1^2/2L_1 - (\Phi_0/2\pi)^2/L_J \cos\left(2\pi \frac{\phi_1 - \phi_{ext}}{\Phi_0}\right). \quad (10)$$

Circuit parameters are to satisfy the following relations: $L_1 \gg L_J$ and $\sqrt{L_J/C_1} \sim R_Q$. The first condition ensures that there are multiple minima in the effective potential seen by the flux coordinate ϕ_1 ; in practice this requires a rather large linear inductance which is achieved by a chain of order 100 larger-area Josephson junctions [29]. The second condition ensures that there is tunneling of the flux between the neighboring wells. The fluxonium-photon interaction Hamiltonian is more conveniently written in the flux gauge and is obtained by analogy with Eq. (2):

$$H_{\text{fluxonium-photon}} = H_{\text{fluxonium}}(\phi_1, Q_1) + Q_2^2/2C_2 + (\phi_1 - \phi_2)^2/2L_2. \quad (11)$$

Let us focus on the specific value of external flux $\phi_{ext} = \Phi_0/2$ for which the atom's effective potential has a symmetric double-well shape consisting of two lowest degenerate local minima separated by approximately the flux quantum Φ_0 . The lowest transition frequency ω_{eg} from the bare ground state to the first excited state is due to the tunneling of the flux variable ϕ_1 between these minima. Physically, this corresponds to a coherent tunneling of flux in and out of the superconducting loop and sometimes is referred to as a quantum phase-slip [37]. The frequency of this tunneling transition can be much lower than the frequency of vibrations in the same well (often called plasma frequency), in which case the spectrum tends to be very anharmonic. It is then tempting to truncate $H_{\text{fluxonium}}$ to its lowest two states $|0\rangle$ and $|1\rangle$ according to the following substitution:

$$\phi_1 \rightarrow \langle 0|\phi_1|1\rangle \sigma_x \quad (12)$$

$$H_{\text{fluxonium}}(\phi_1, Q_1) \rightarrow \frac{1}{2} \hbar \omega_{01} \sigma_z. \quad (13)$$

By making this substitution into the atom-photon Hamiltonian (11), relabeling $\omega_2 \rightarrow \omega_r$, $a_1 \rightarrow a$, and $Z_2 \rightarrow Z_r$ and using the fact that $\sigma_x^2 = 1$ we indeed obtain an effective quantum Rabi model with the dimensionless coupling constant (see Eq. (1))

$$\frac{g}{\omega_r} = \frac{2\langle 0|\phi_1|1\rangle}{\Phi_0} \times x \quad (14)$$

where $x = \frac{1}{2}\sqrt{\pi R_Q/Z_r}$ is independent of the atom spectral details. For a typical fluxonium circuit $\langle 0|\phi_1|1\rangle \approx \Phi_0/2$ implying $g/\omega_r \approx x$. Therefore, a coupling strength $x > 1$ can be readily implemented using $Z_r \sim 50 \, \Omega$ resonance circuits [21]. Comparing Eq. (14) to the expression for x for linear circuits (see Table II) we can formally assign to fluxonium circuit the effective impedance $Z_{\text{fluxonium}} \approx \pi R_Q$.

B. Cooper pair box atom

Maximally strong coupling of a Cooper pair box circuit to a resonator is also achieved by shunting it with a series LC -circuit. Formally this is equivalent to removing the linear inductance L_1 from the fluxonium circuit (Fig. 2b). The resulting circuit contains an "island", i.e. a superconducting region, whose total charge is quantized and can only change by a tunneling of a Cooper pair. This island can be additionally voltage-biased (not shown) to create an offset charge Q_{ext} . The Hamiltonian of this system, called a Cooper pair box (CPB) atom, is given by

$$H_{\text{CPB}}(\phi_1, Q_1) = (Q_1 + Q_{\text{ext}})^2/2C_1 - E_J \cos(2e\phi_1/\hbar). \quad (15)$$

The operator Q_1 has integer eigenvalues in units of $2e$ and its conjugate flux ϕ_1 is a compact variable defined on the interval $[0, \hbar/2e)$. Consequently, the flux-charge commutation relation here changes to $\exp(iq\phi_1/\hbar)Q_1 \exp(-iq\phi_1/\hbar) = Q_1 + q$. The atomic spectrum can be understood as that of a particle in a periodic cosine potential with a quasi-momentum given by the offset charge Q_{ext} [38]. The atom-photon coupling in this case is more conveniently written in the charge gauge, by analogy with Eq. (3):

$$H_{\text{CPB-photon}} = H_{\text{CPB}}(\phi_1, Q_1 + Q_2) + Q_2^2/2C_2 + \phi_2^2/2L_2. \quad (16)$$

In this gauge the Q_2^2 -term coming from $H_{\text{CPB}}(\phi_1, Q_1 + Q_2)$ strongly renormalizes the resonator frequency. It turns out that the analysis appears more intuitive if we take into account this renormalization explicitly. Physically, this corresponds to replacing the resonator capacitance C_2 with a parallel combination $C_1||C_2 = C_1C_2/(C_1 + C_2)$. This is particularly evident in the limit $E_J \rightarrow 0$. To quantize the oscillator we introduce the renormalized resonator frequency $\omega_r = 1/\sqrt{L_2C_1||C_2}$, the renormalized resonator impedance $Z_r = \sqrt{L_2/C_1||C_2}$, and the associated annihilation operator a to obtain:

$$H_{\text{CPB-photon}} = H_{\text{CPB}}(\phi_1, Q_1) + \hbar\omega_r a^\dagger a + \hbar\omega_r \frac{C_2}{C_1 + C_2} \sqrt{\pi Z_r/R_Q} \times i(a^\dagger - a) \frac{Q_1}{2e}. \quad (17)$$

For $Q_{\text{ext}} = -e$, the charging energy of the Cooper pair box is degenerate for $Q/2e = 0, 1$. The Josephson term lifts the degeneracy by tunneling of Cooper pairs. If we truncate the Hamiltonian (17) to the two lowest atomic states $|0\rangle$ and $|1\rangle$, we get

$$Q_1 \rightarrow \langle 0|Q_1|1\rangle \sigma_z, \quad (18)$$

$$\cos(2e\phi_1/\hbar) \rightarrow \frac{\sigma_x}{2}. \quad (19)$$

This truncation gives a quantum Rabi model (see Eq. 1) with the dimensionless coupling constant g

$$\frac{g}{\omega_r} = \frac{C_2}{C_1 + C_2} \times \frac{\langle 0|Q_1|1\rangle}{e} \times x, \quad (20)$$

where this time $x = \frac{1}{2}\sqrt{\pi Z_r/R_Q}$. For typical CPB parameters, $\langle 0|Q_1|1\rangle/e \sim 1$, so as long as we choose $C_1 \ll C_2$, we get a particularly simple result $g/\omega_r \approx x$. To go beyond strong coupling, we need a series circuit with a large inductance L_2 , such that $Z_r \approx \sqrt{L_2/C_1} \sim R_Q$. Interestingly, capacitance C_2 is irrelevant as long as $C_1 \ll C_2$. This is a consequence of properly taking into account the " A^2 "-like term in writing Eq. (16). Taking the typical small junction capacitance value $C_1 \approx 1 \, \text{fF}$ and the largest demonstrated linear inductance $L_2 \approx 300 \, \text{nH}$, we get $Z_r \approx 17 \, \text{k}\Omega$ [29] and $x \approx 1.5$, sufficient to reach the ultrastrong coupling regime with a charge qubit.

Atom/Parameter	ω_r	Z_r	g/ω_r	x
Fluxonium	$1/\sqrt{L_2 C_2}$	$\sqrt{L_2/C_2}$	$\frac{2\langle e \phi_1 g\rangle}{\Phi_0} \times x$	$\frac{1}{2}\sqrt{\pi R_Q/Z_r}$
Cooper pair box	$1/\sqrt{L_2 C_1 C_2/(C_1 + C_2)}$	$\sqrt{L_2(C_1 + C_2)/C_1 C_2}$	$\frac{C_2}{C_1 + C_2} \frac{\langle e Q_1 g\rangle}{e} \times x$	$\frac{1}{2}\sqrt{\pi Z_r/R_Q}$

TABLE II. Parameters of the quantum Rabi model as a result of the two-level truncation for the two types of circuit atoms considered in the text. They depend on the circuit inductances/capacitances (Fig. 2) and on the flux/charge matrix elements between the bare atom ground state and the first excited state.

IV. NUMERICAL DIAGONALIZATION OF MULTILEVEL CIRCUIT HAMILTONIANS

The two-level truncation for both circuit atoms yielded a quantum Rabi model with $g/\omega_r > 1$ for realistic circuit parameters. Are we allowed to perform such a truncation? What is the role of higher atomic levels in the ultrastrong coupling regime? To answer this question we compare the results of the numerical simulation of the Hamiltonians (11,16) keeping over 100 atom and resonator levels to the prediction of their truncated quantum Rabi model implementations. It is convenient in our simulations to describe circuit parameters using energy scales given by $E_C = e^2/2C$ for a capacitance C , $E_L = (\Phi_0/2\pi)^2/L$ for an inductance L , and $E_J = (\Phi_0/2\pi)^2/L_J$ for the Josephson junction. In presenting results, we will measure these energies and circuit transition frequencies in units of GHz.

A. Frequency spectra for the fluxonium-resonator circuit

The three numbers E_J , E_{L_1} , and E_{C_1} , together with the external flux ϕ_{ext} define the fluxonium transition spectrum. We chose a set $(E_J, E_{C_1}, E_{L_1}) = (5, 5, 0.5)$ GHz which is experimentally realistic and yields a highly anharmonic spectrum with $\omega_{01}/2\pi \approx 2.47$ and $\omega_{02} > 3 \times \omega_{01}$. We consider a conventional resonant case ($\omega_r/2\pi = 2.47$) and two off-resonant cases ($\omega_r/2\pi = 8, 20$). The case $\omega_r/2\pi = 8$ is special because then $\omega_{12} \approx \omega_r$, while $\omega_r/2\pi = 20$ represent a high-frequency limit of $\omega_r \gg \omega_{01}$.

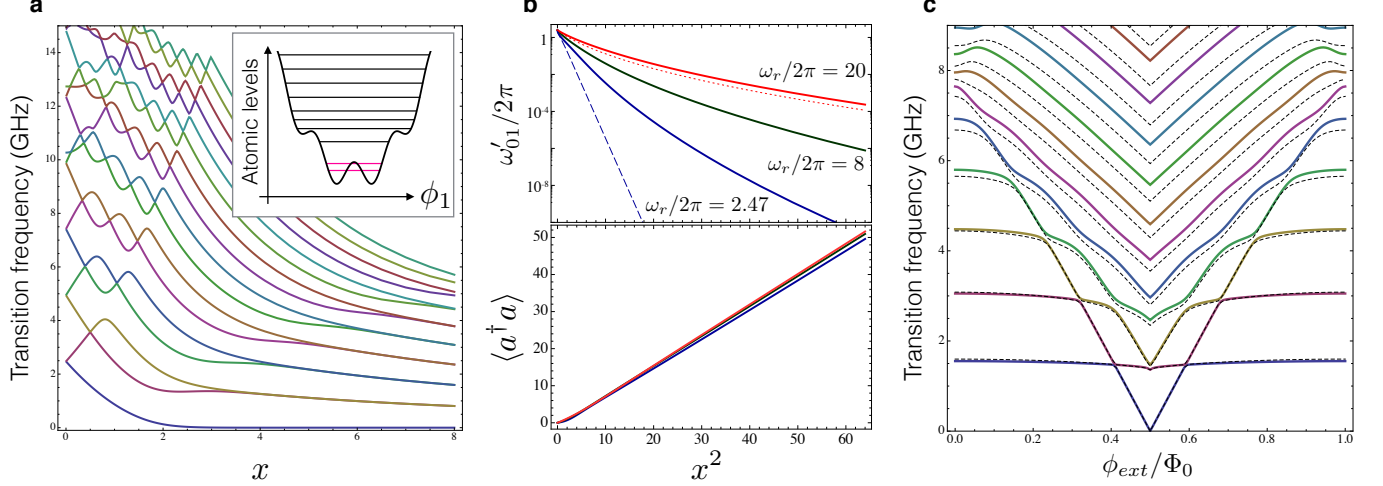


FIG. 3. (a) Transition spectrum of the Hamiltonian (11) including over 100 atom and 100 photon levels for $\omega_r = \omega_{01} = 2.47$. The fluxonium atom parameters are $(E_J, E_{C_1}, E_{L_1}) = (5, 5, 0.5)$. Inset shows the spectrum of the bare (uncoupled) atom levels within the flux-dependent potential. (b-top) Frequency splitting ω'_{01} between the ground state and the first excited state for three bare photon frequencies, $\omega_r = 2.47$ (blue), $\omega_r = 8$ (dark green) and $\omega_r = 20$ (red). Dashed blue line is the result of the quantum Rabi model, dotted red line is the result with $L_2 = 0$ (a capacitively shunted fluxonium model). (b-bottom) Expectation value of the photon number in the ground state for the same three resonator frequencies. (c) Transition spectrum of Hamiltonian (11) as a function of the external flux for $x = 4$ (solid lines) and spectrum of the uncoupled fluxonium with renormalized parameters (dashed lines).

Our numerical simulations show that while the spectrum of a fluxonium coupled to a single-mode photon is indeed qualitatively similar to that of the quantum Rabi model, there are several striking differences (Fig. 3). The features similar to the quantum Rabi model are: (i) the spectrum at $x \gg 1$ reduces to a harmonic ladder of nearly degenerate

pairs of levels (Fig. 3a) and (ii) the expectation of the number of photons in the resonator in the ground state grows as x^2 , being insensitive to the value of the resonator frequency (Fig. 3b - bottom). The key discrepancy from the quantum Rabi model are: (I) the frequency gap between nearly degenerate level doublets reduces algebraically with x as opposed to the prediction of being x -independent for $x \gg 1$ and (II) the even-odd ground state splitting scales sub-exponentially with x^2 (or, equivalently, sub-exponentially with the number of ground state photons). Furthermore, the ground-states splitting reduces by orders of magnitude if the resonator frequency increases (Fig. 3b).

We now offer a physical interpretation to our numerical results. We first discuss the quadratic growth of ground-state photons as a function of the dimensionless coupling x . It can be estimated from the amount of displacement of the oscillator by the atom. If we disregard tunneling, the oscillator is displaced approximately by $\pm\Phi_0/2$. This corresponds to the coherent state amplitude $\alpha = \Phi_0/(\langle 0|\phi_2^2|0\rangle)^{1/2}$, which happens to equal exactly x , such that the ground state photon number is given by $\langle a^\dagger a \rangle = x^2$. Quantum tunneling of the atomic coordinate merely entangles the two oppositely displaced oscillator states and does affect the ground-state photon number. Next, we turn to the spectral features of the Hamiltonian (11). Why does the scaling of the lowest transition frequency deviate so much from the predictions of the quantum Rabi model? To understand this, let us consider an atomic transition between states 0 and 1 and calculate to second order in x its shift χ_{01} due to the interaction with a cavity. We will also assume no resonance conditions, i.e. $\omega_{01} \neq \omega_r$. The answer is given by

$$\chi_{01} = x^2 \omega_r^2 \sum_{i \neq 0} \frac{2\omega_{0i}^2}{\omega_{0i}^2 - \omega_r^2} |\langle 0|2\phi_1/\Phi_0|i\rangle|^2 - x^2 \omega_r^2 \sum_{j \neq 1} \frac{2\omega_{1j}^2}{\omega_{1j}^2 - \omega_r^2} |\langle 1|2\phi_1/\Phi_0|j\rangle|^2. \quad (21)$$

This expression for χ_{01} can differ greatly from its 2-level truncated version (the terms $i = 1, j = 0$) if there are transitions from either state 0 or 1 to higher atomic states with non-zero matrix elements and with frequencies close to the resonator frequency. In other words, already in second order in x , the shift χ_{01} can be large even if $\langle 0|2\phi_1/\Phi_0|1\rangle = 0$ and $\omega_{01} \ll \omega_r$. Clearly truncation to the two states is even more dangerous for $x \gg 1$, no matter how anharmonic the atomic spectrum is.

Although perturbation theory fails at $x \gg 1$ we can still make sense of the low-energy spectrum in the high photon frequency limit $\omega_r \gg \omega_{01}$. In this limit it is tempting to just ignore a voltage drop across the inductance L_2 thus reducing the effect of the resonator to simply shunting the qubit with the capacitance C_2 ; mind that to get $x \gg 1$ one needs $C_2 \gg C_1$. As a result, flux tunneling is suppressed since the capacitance plays the role of a mass for the tunneling of the flux coordinate ϕ_1 . This suppression is similar to the familiar suppression of macroscopic quantum tunneling of phase in large-capacitance Josephson junction [32]. The WKB approximation predicts that the tunnel splitting will scale exponential in $\sqrt{C_2}$ which is proportional to x if we keep the resonator frequency constant while increasing the coupling. Our numerical calculation, where we ignore the inductance L_2 (Fig. 3b, red dotted line) agrees well with the full numerical simulation using $\omega_r = 20$ and $\omega_{01} = 2.47$ (Fig. 3b, red solid line).

Finally, we observe that the energy spectrum of a quantum Rabi model at large couplings is qualitatively very similar to the spectrum of a single fluxonium atom with an enhanced ratio E_J/E_{C_1} (large barrier, heavy mass). The flux particle can semi-classically vibrate in either left or right wells which creates the 2-fold degeneracy in the spectrum. Exponentially small tunneling through the barrier weakly lifts the degeneracy. In other words, the main effect of ultrastrong coupling of a fluxonium (or a flux qubit) to a cavity, from a low-energy spectroscopic point of view, reduces to a simple suppression of coherent flux tunneling. To illustrate this point, we fix $x = 4$, deep in the non-perturbative coupling regime, and simulate the spectrum of Eq. (11) as a function of flux ϕ_{ext} . The resulting spectrum (Fig. 3c, solid lines), when restricted to the lowest few states is remarkably similar to that of a bare fluxonium with renormalized parameters (Fig. 3c, dashed lines). The difference between the two models can only be found in quantitative discrepancy of the higher-frequency transitions.

B. Frequency spectra for the Cooper pair box circuit

Our results for the Cooper pair box are summarized in Fig. (4). In contrast to the fluxonium case, here the full model shows very minor discrepancy from the truncated quantum Rabi model. We have fixed the capacitances C_1 and C_2 such that $E_{C_1} = 10$, typical for a small-capacitance tunnel junction, and $E_{C_2} = 1$ in order to respect the condition $C_1 \ll C_2$. We varied the coupling x by varying L_2 (see Table II and discussion in the text): this also varies the bare photon frequency, but we think that this choice is the most experimentally relevant. We show the results for two different values of the Josephson energy: $E_J = 2$ (Fig. 4a,b), representing stronger anharmonicity and $E_J = 5$ (Fig. 4c,d), representing weaker anharmonicity.

Our main finding is that the low-energy spectrum of the coupled atom-photon system can essentially be understood as a suppression of E_J exponentially in x^2 irrespectively on the amount of anharmonicity of the bare atom. This

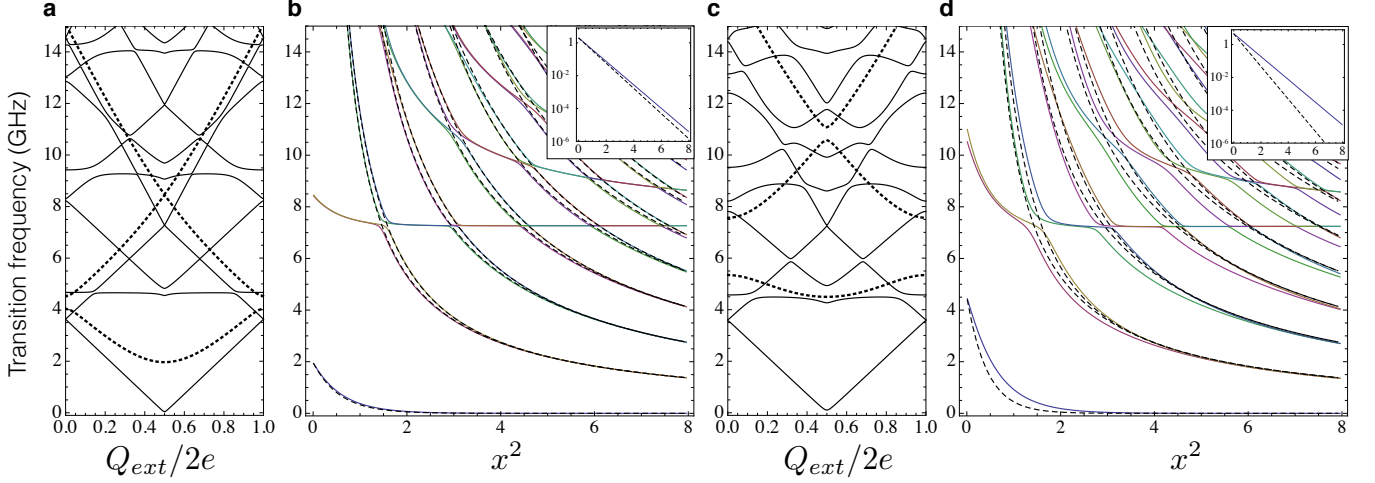


FIG. 4. (a) Transition spectrum of the bare Cooper pair box (Eq. 15) (dashed lines) and coupled Hamiltonian (Eq. 16) (solid lines) as a function of offset charge for the parameters $(E_J, E_{C_1}, E_{L_2}, E_{C_2}) = (2, 10, 0.25, 1)$. (b) Transition spectrum of the coupled Hamiltonian (Eq. 16) (solid lines) and its 2-level quantum Rabi model (dashed lines) as a function of the dimensionless coupling parameter x . Parameter E_{L_2} was varied while other parameters were kept constant. Inset shows the lowest transition frequency on the log scale for both models. (c) Same as (a) for $E_J = 5$. (d) Same as (b) for $E_J = 5$.

is particularly evident in the case $(E_J, E_{C_1}) = (2, 10)$ (Fig. 4a), where one can recognize spectral lines of a Cooper pair box with $E_J \sim 0$. Higher atomic transitions almost do not interact with the rest of the spectrum (Fig. 4b). Scaling of the lowest transition frequency with x^2 essentially coincides with the quantum Rabi model's result over many orders of magnitude. The effect of higher CPB levels is more prominent in case of the less anharmonic atom $(E_J, E_{C_1}) = (5, 10)$, where the lowest bare atomic transition is almost charge-insensitive, like in the transmon qubit. Naively, one would expect a drastic departure from the quantum Rabi model, because the second atomic transition frequency is very close to the first one (Fig. 4c - dashed lines). Nevertheless, the lowest transition frequency still scales exponentially with x^2 and the deviation from the quantum Rabi model is only in the renormalization of the coupling constant by a factor of order unity (Fig. 4b - inset).

Such *insensitivity* of the Cooper pair box circuit to its higher levels, even when $x \gg 1$ and when E_J/E_{C_1} is not small (approaching the transmon regime) is likely due to a rapid suppression of the charge transition dipole matrix element with the level number. The main spectral feature of the ultrastrong coupling for a charge qubit - the exponential in x^2 suppression of E_J at $x \gg 1$ - can be qualitatively understood as dressing of a Cooper pair with a cloud of virtual photons, whose size grows with the coupling constant. As a result of this dressing, coherent Cooper pair tunneling is suppressed when $x \gg 1$. Indeed, the width of the ground state wavefunction of the uncoupled oscillator is given by $\langle 0 | (Q_2/2e)^2 | 1 \rangle^{1/2} \sim 1/x$ in the charge representation. Since tunneling of a Cooper pair shifts the oscillator's charge variable $Q_2/2e$ by a unity, this process will be suppressed exponentially in x^2 due to a small Frank-Condon overlap of the oscillator states before and after the tunneling event. Thus, unlike the suppression of flux tunneling in fluxonium, renormalization of E_J here cannot be explained by a simple capacitive (or inductive) loading of the junction. In fact, the physics of ultrastrong coupling of a charge qubit to a single-mode photon appears to be very similar to dynamical Coulomb blockade, which describes the non-linearity of the inelastic charge-transport in tunnel junctions coupled to a high-impedance leads [39].

C. Entanglement spectrum of the ground state

To characterize the entanglement between atom and resonator in the ground state, a very useful quantity is the entanglement spectrum [40]. Let us call $|G\rangle$ the ground state of a bipartite system where A and B are the two partitions. We can define a pure state density-matrix $\rho = |G\rangle\langle G|$ for the ground state. By partial trace with respect to subsystem B , we get the reduced density matrix for the subsystem A , namely $\rho_A = \text{Tr}_B(\rho)$. An useful quantity is the entanglement spectrum, that is the spectrum of eigenvalues of the reduced density matrix. The reduced density matrix is a hermitian operator, hence it can be diagonalized by an orthonormal basis of eigenstates $|\Psi_r^{(A)}\rangle$ with

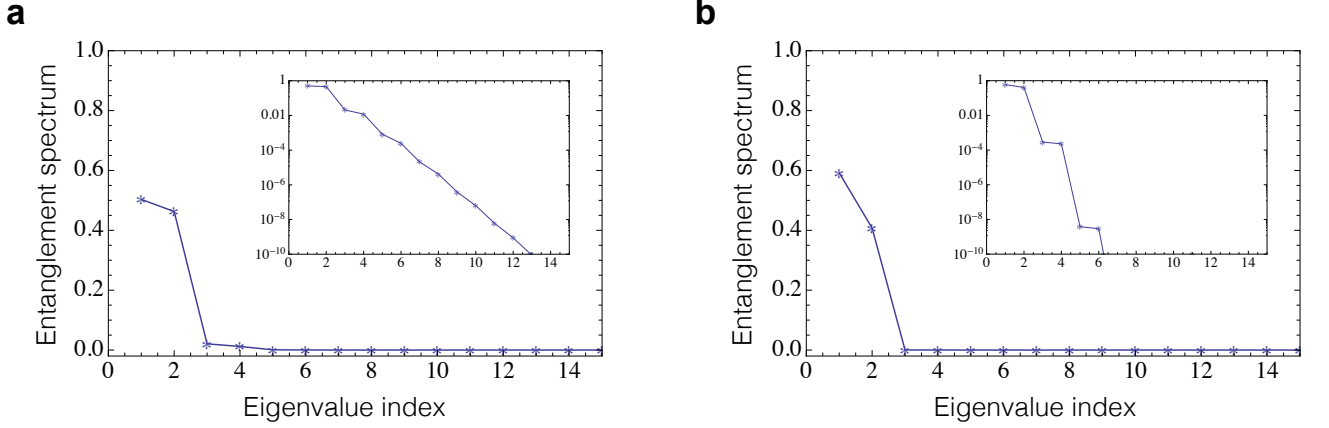


FIG. 5. Entanglement spectrum for the atom-resonator system. (a) Results for a fluxonium circuit (parameters as in Fig. 3, $x = 4$). (b) Results for a Cooper pair box (same parameters as in Fig. 4c).

eigenvalues $0 \leq p_r \leq 1$ such that $\sum_r p_r = 1$, namely

$$\rho_A = \sum_r p_r |\Psi_r^{(A)}\rangle \langle \Psi_r^{(A)}|. \quad (22)$$

The entanglement spectrum is just the set of probabilities $\{p_r\}_r$. For a separable state (no entanglement), the reduced density matrix corresponds to a pure state, namely $p_1 = 1$ and $p_{r \neq 1} = 0$: in other words, the entanglement spectrum is a point.

In the quantum Rabi model, when $g \gg \omega_r = \omega_{eg}$ the ground state tends asymptotically to the Schrodinger cat state:

$$|G_{Q-Rabi}\rangle \simeq \mathcal{N}(|\alpha\rangle |\leftarrow\rangle - |-\alpha\rangle |\rightarrow\rangle) \quad (23)$$

where $|\alpha\rangle$ is a coherent state for the resonator with amplitude $\alpha = g/\omega_r$, $\sigma_x |\rightarrow\rangle = |\rightarrow\rangle$ and $\sigma_x |\leftarrow\rangle = -|\leftarrow\rangle$. The coefficient \mathcal{N} is the normalization constant. For $|\alpha| \gg 1$, the entanglement spectrum associated to the ground state in Eq. (23) is $\{p_1 = 1/2, p_2 = 1/2\}$.

In Fig. 5 we show results for the entanglement spectrum for the ground state of the fluxonium circuit (left panel) and for the Cooper pair box case (right panel). For both circuits we have considered a large dimensionless coupling $x = 4$. In both cases, the entanglement spectrum is dominated by two nearly equal eigenvalues, similarly to the quantum Rabi model case. In the inset, the eigenvalues are plotted in log scale to see the other and much smaller eigenvalues $p_{r \geq 3} \ll 1$. It is clear that in the fluxonium case there are some minor deviations with respect to the simple entanglement spectrum of the quantum Rabi model. Such deviations are even smaller for the Cooper pair box as the other eigenvalues are smaller by several orders of magnitude. Indeed, the Cooper pair box provides a very close match to the ideal quantum Rabi model also for very large values of the dimensionless coupling x .

Which is the physical interpretation of such simple entanglement spectrum with two dominant eigenvalues for the multilevel circuit atom? If we partially trace the pure ground state density-matrix with respect to the resonator degrees of freedom, one obtains a reduced density matrix ρ_{at} for the atomic system. A mixed density matrix ρ_{at} implies entanglement between the atom and the resonator. In the quantum Rabi model, the dimension of the atomic Hilbert space is two, so trivially there are only two possible eigenvalues and two corresponding atomic eigenstates. Maximum entanglement is achieved when $p_1 = p_2 = 1/2$. In a multilevel atom instead it is not trivial at all that the entanglement spectrum is dominated by *only two* eigenvalues. The corresponding eigenvectors do define an effective two-level description, although they are not at all the bare atomic states. We have verified (not shown) that the most probable eigenstates of the atomic reduced density matrix ρ_{at} (corresponding to the two dominant eigenvalues $p_1 \approx p_2 \approx 1/2$ in Fig. 5) are linear superpositions of *many* bare atomic states.

V. SUMMARY AND OUTLOOK

In conclusion, we have investigated theoretically two classes of superconducting circuits where an artificial atom – a fluxonium and a Cooper pair box – is coupled to a lumped-element *LC*-resonator. Our studies of the fluxonium atom

cover qualitatively the case of the 3–4 junction flux qubit, while the studies of a Cooper pair box included a relatively large E_J/E_C ratio characteristic of a transmon regime. We first derived and quantized circuit Hamiltonians in various gauges following Ref. [34], assuming an arbitrary coupling strength, and fully taking into account " A^2 "-like terms. To achieve the regime $g/\omega_r > 1$ we found that a low-impedance resonator is required in case of flux tunneling, which is consistent with the previous studies [18, 27], and a high-impedance resonator is required for charge tunneling. The impedance scale is defined by the resistance quantum for Cooper pairs $R_Q = h/(2e)^2$. We then numerically explored spectral features of our Hamiltonians taking into account a large number of bare atom and photon states, a study that was not previously made for either circuit.

Despite significant deviation of both circuits from two-level systems, many essential aspects of the quantum Rabi model were recovered in the limit $g/\omega_r \gg 1$. Those include the entangled atom-photon structure of the ground state with a lifting of the ground state degeneracy that rapidly vanishes as g/ω_r grows and becomes larger than unity, and a nearly harmonic excitation spectrum. The ground state degeneracy is lifted exponentially in $(g/\omega_r)^2$ in case of the Cooper pair box circuit, which coincides with the quantum Rabi model's prediction, while significant order of magnitude corrections were found for the fluxonium. The deviation is particularly notable when the bare photon frequency ω_r matches some of the higher transitions of the bare atom, such as ω_{02} or ω_{12} .

Physical interpretation of ultrastrong coupling regime, $g/\omega_r \gg 1$, for both flux and charge tunneling circuits is worth a separate note. In case of fluxonium (or a flux qubit), the main effect, is the suppression of flux tunneling. The origin of suppression is evident in the high photon frequency case, $\omega_r \gg \omega_{01}$: one can simply ignore resonator's inductance and treat the overcoupled atom-oscillator system as a fluxonium (or flux qubit) shunted by the large capacitance of the low-impedance LC -circuit. As a result, the flux tunneling is suppressed by analogy with the suppression of macroscopic quantum tunneling of phase in large-capacitance Josephson junctions [32]. In case of the Cooper pair box circuit, the main effect is the suppression of Cooper pair tunneling, irrespective of the amount of anharmonicity of the bare circuit. Here, the suppression is of the Frank-Condon type and cannot be explained by a linear circuit elements renormalization. The suppression of E_J by a high-impedance resonator environment draws analogies to the dynamical Coulomb blockade of charge transport in small-capacitance tunnel junction [39].

How come basic spectral features of the quantum Rabi model survive in both types of multi-level circuit atoms at $g/\omega_r \gg 1$? We believe the answer lies in the intrinsic "two-levelness" of both circuits when they are maximally frustrated by external flux/charge. The motion of flux and charge variables between their two semiclassical values (zero or one flux quanta in the loop/zero or one charge quantum on the island) couples to the boson field, giving rise to an effective quantum Rabi dynamics, even though accurate description of this motion requires taking into account a large number of bare atomic levels. In other words, it is not the strong anharmonicity of the flux qubit that is required to observe quantum Rabi dynamics with this circuit at $g/\omega_r \gg 1$. Instead the key is the symmetric double-well potential seen by the flux degree of freedom, which is essentially a classical property of this circuit. Similar reasoning holds for the charge states of a superconducting island.

Our theoretical results seem encouraging for further experimental exploration of the physics of the quantum Rabi model with arbitrary large coupling. Although spectral features of ultrastrong qubit-oscillator system are relatively straightforward to observe [21], study of coherent quantum Rabi dynamics might be more challenging. Most notably, at large g/ω_r , both charge and flux circuits become first-order sensitive to charge and flux noise respectively, which would limit coherence times to only few nanoseconds for charge and flux qubits. This is partially mitigated in case of fluxonium, where a large loop inductance results in first-order flux-noise decoherence in excess of 1 μs [37, 41]. Non-destructive measurement of the non-trivial ground state properties can be done for example using an ancillary qubit [42, 43]. An efficient release of ground state photons (the so-called radiation from the vacuum) can occur only if the system parameters are changed in a non-adiabatic fashion [44–48], which can probably be achieved using a fast flux/charge modulation in the circuits considered here.

ACKNOWLEDGMENTS

V.E.M. acknowledges support from the US National Science Foundation (DMR-1455261) and from the Alfred P. Sloan Research Fellowship (FG-2015-66004). A.B. acknowledges support from the Air Force Office of Scientific Research. C. C. acknowledges support from ERC (via the Consolidator Grant "CORPHO" No. 616233).

-
- [1] A. Wallraff, D. I. Schuster, A. Blais, L. Frunzio, R. S. Huang, J. Majer, S. Kumar, S. M. Girvin, and R. J. Schoelkopf, *Nature* **431**, 162 (2004).
 - [2] R. J. Schoelkopf and S. M. Girvin, *Nature* **451**, 664 (2008).

- [3] M. H. Devoret and R. Schoelkopf, *Science* **339**, 1169 (2013).
- [4] J. M. Raimond, M. Brune, and S. Haroche, *Rev. Mod. Phys.* **73**, 565 (2001).
- [5] E. T. Jaynes and F. W. Cummings, *Proceedings of the IEEE* **51**, 89 (1963).
- [6] I. I. Rabi, *Phys. Rev.* **49**, 324 (1936).
- [7] I. I. Rabi, *Phys. Rev.* **51**, 652 (1937).
- [8] D. Braak, *Phys. Rev. Lett.* **107**, 100401 (2011).
- [9] C. Ciuti, G. Bastard, and I. Carusotto, *Phys. Rev. B* **72**, 115303 (2005).
- [10] P. Nataf and C. Ciuti, *Phys. Rev. Lett.* **104**, 023601 (2010).
- [11] J. Casanova, G. Romero, I. Lizuain, J. J. García-Ripoll, and E. Solano, *Phys. Rev. Lett.* **105**, 263603 (2010).
- [12] S. Ashhab and F. Nori, *Phys. Rev. A* **81**, 042311 (2010).
- [13] A. Baksic and C. Ciuti, *Phys. Rev. Lett.* **112**, 173601 (2014).
- [14] A. P. Hines, C. M. Dawson, R. H. McKenzie, and G. Milburn, *Physical Review A* **70**, 022303 (2004).
- [15] P. Nataf and C. Ciuti, *Phys. Rev. Lett.* **107**, 190402 (2011).
- [16] N. K. Langford, R. Sagastizabal, M. Kounalakis, C. Dickel, A. Bruno, F. Luthi, D. J. Thoen, A. Endo, and L. DiCarlo, *arXiv:1610.10065* (2016).
- [17] A. Mezzacapo, U. Las Heras, J. S. Pedernales, L. DiCarlo, E. Solano, and L. Lamata, *Scientific Reports* **4**, 7482 (2014).
- [18] M. Devoret, S. Girvin, and R. Schoelkopf, *Annalen der Physik* **16**, 767 (2007).
- [19] P. Forn-Díaz, J. Lisenfeld, D. Marcos, J. J. García-Ripoll, E. Solano, C. J. P. M. Harmans, and J. E. Mooij, *Phys. Rev. Lett.* **105**, 237001 (2010).
- [20] T. Niemczyk, F. Deppe, H. Huebl, E. Menzel, F. Hocke, M. Schwarz, J. Garcia-Ripoll, D. Zueco, T. Hümmer, E. Solano, *et al.*, *Nature Physics* **6**, 772 (2010).
- [21] F. Yoshihara, T. Fuse, S. Ashhab, K. Kakuyanagi, S. Saito, and K. Semba, *arXiv preprint arXiv:1602.00415* (2016).
- [22] P. Nataf and C. Ciuti, *Nature communications* **1**, 72 (2010).
- [23] O. Viehmann, J. von Delft, and F. Marquardt, *Physical Review Letters* **107**, 113602 (2011).
- [24] T. Jaako, Z.-L. Xiang, J. J. Garcia-Ripoll, and P. Rabl, *Physical Review A* **94**, 033850 (2016).
- [25] M. Bamba, K. Inomata, and Y. Nakamura, *Phys. Rev. Lett.* **117**, 173601 (2016).
- [26] M. Malekakhlagh and H. E. Türeci, *Phys. Rev. A* **93**, 012120 (2016).
- [27] J. Bourassa, J. M. Gambetta, A. A. Abdumalikov, O. Astafiev, Y. Nakamura, and A. Blais, *Phys. Rev. A* **80**, 032109 (2009).
- [28] J. J. Hopfield, *Phys. Rev.* **112**, 1555 (1958).
- [29] V. E. Manucharyan, J. Koch, L. I. Glazman, and M. H. Devoret, *Science* **326**, 113 (2009), <http://science.sciencemag.org/content/326/5949/113.full.pdf>.
- [30] Y. Nakamura, Y. A. Pashkin, and J. S. Tsai, *Nature* **398**, 786 (1999).
- [31] J. Koch, T. M. Yu, J. Gambetta, A. A. Houck, D. I. Schuster, J. Majer, A. Blais, M. H. Devoret, S. M. Girvin, and R. J. Schoelkopf, *Physical Review A* **76**, 042319 (2007).
- [32] J. Clarke, A. Cleland, M. H. Devoret, D. Esteve, and J. Martinis, *Science* **239**, 992 (1988).
- [33] M. H. Devoret, D. Esteve, H. Grabert, G.-L. Ingold, H. Pothier, and C. Urbina, *Physical review letters* **64**, 1824 (1990).
- [34] M. H. Devoret, *Les Houches, Session LXIII* (1995).
- [35] A. A. Anappara, S. De Liberato, A. Tredicucci, C. Ciuti, G. Biasiol, L. Sorba, and F. Beltram, *Phys. Rev. B* **79**, 201303 (2009).
- [36] Y. Todorov, A. M. Andrews, R. Colombelli, S. De Liberato, C. Ciuti, P. Klang, G. Strasser, and C. Sirtori, *Physical Review Letters* **105**, 196402 (2010).
- [37] V. E. Manucharyan, N. A. Masluk, A. Kamal, J. Koch, L. I. Glazman, and M. H. Devoret, *Physical Review B* **85**, 024521 (2012).
- [38] V. Bouchiat, D. Vion, P. Joyez, D. Esteve, and M. H. Devoret, *Physica Scripta* **1998**, 165 (1998).
- [39] H. Grabert and M. H. Devoret, eds., *Single Charge Tunneling* (Plenum, New York, 1992).
- [40] H. Li and F. D. M. Haldane, *Phys. Rev. Lett.* **101**, 010504 (2008).
- [41] A. Kou, W. Smith, U. Vool, R. Brierley, H. Meier, L. Frunzio, S. Girvin, L. Glazman, and M. Devoret, *arXiv preprint arXiv:1610.01094* (2016).
- [42] J. Lolli, A. Baksic, D. Nagy, V. E. Manucharyan, and C. Ciuti, *Phys. Rev. Lett.* **114**, 183601 (2015).
- [43] S. Felicetti, T. Douce, G. Romero, P. Milman, and E. Solano, *Scientific reports* **5**, 11818 (2015).
- [44] C. Ciuti and I. Carusotto, *Phys. Rev. A* **74**, 033811 (2006).
- [45] S. D. Liberato, C. Ciuti, and I. Carusotto, *Phys. Rev. Lett.* **98**, 103602 (2007).
- [46] S. De Liberato, D. Gerace, I. Carusotto, and C. Ciuti, *Phys. Rev. A* **80**, 053810 (2009).
- [47] G. Günter, A. A. Anappara, J. Hees, A. Sell, G. Biasiol, L. Sorba, S. De Liberato, C. Ciuti, A. Tredicucci, A. Leitenstorfer, *et al.*, *Nature* **458**, 178 (2009).
- [48] B. Peropadre, P. Forn-Díaz, E. Solano, and J. J. García-Ripoll, *Physical Review Letters* **105**, 023601 (2010).